Temperature-induced exciton switching in long alkyl chain based inorganic-organic hybrids

K. Pradeesh,[1,a)] J. J. Baumberg,[2] and G. Vijaya Prakash[1]
[1]*Nanophotonics lab, Department of Physics, Indian Institute of Technology Delhi, New Delhi, 110016, India*
[2]*Nanophotonics Centre, Cavendish Laboratory, University of Cambridge, Cambridge, CB3 0HE, United Kingdom*

(Received 16 August 2011; accepted 5 December 2011; published online 6 January 2012)

Photoluminescence and transmission is systematically explored in thin films of long–alkyl-chain-based inorganic-organic (IO) hybrids $(C_nH_{2n+1}NH_3)_2PbI_4$ (n = 12, 16, 18) (CnPI) and $NH_3C_{12}H_{22}NH_3PbI_4$ (DDPI). Such IO-hybrids, which form natural multiple quantum well structures stacked up along c-axis, possess strong room-temperature exciton transitions. These hybrids exhibit reversible phase transition of two different crystal phase transitions at easily accessible device temperatures. Flipping the structural phase is clearly reflected in switching of the excitons with corresponding photoluminescence and transmission changes showing clear thermal hysteresis. The phase-dependent switching of excitons is predominantly due to reversible crumpling of the inorganic PbI sheet networks. Systematic temperature dependent studies establish a correlation between the structure and optical exciton features. Such thermo-optic exciton switching suggests possible new photonic devices. © *2012 American Institute of Physics*. [doi:10.1063/1.3674324]

I. INTRODUCTION

Inorganic-Organic (IO) hybrid semiconductors provide significant opportunities as multi-functional materials for many electronic and optoelectronic applications. These include inorganic-organic light emitting diodes, inorganic-organic field-effect transistors, and nonlinear optical switches based on strong exciton-photon coupling in microcavity photonic architectures.[1–4] The basic structure of these lead (II) halide-based two-dimensional (2D) pervoskites takes the general form $(R\text{-}NH_3)_2PbI_4$ and $(NH_3\text{-}R\text{-}NH_3)PbI_4$ (where R is organic) consisting of layers of corner-sharing lead iodide octahedra with mono-/bi-layers of organic cations stacked between the inorganic layers.[5–10] These form 'natural' multiple-quantum-well structures (MQWs), where 'wells' of the 2D inorganic semiconducting layer are clad by 'barriers' of the wider bandgap organic layers. Due to the low dimensionality and the contrast in the bandgap of organic and inorganic layers, carriers are confined within the inorganic layers. A large dielectric mismatch (giving dielectric confinement) combined with the quantum confinement between the layers, enables formation of stable excitons with large binding energy even at room-temperatures.[11–13] These IO-hybrids exhibit narrow and strong excitonic absorption and emission features favorable for optoelectronics applications. Such hybrids are thermally stable up to 200 °C and a wide range of structures can be conveniently synthesized by choosing an appropriate intercalating organic moiety.[8,9,14] Of particular focus here is the observation of reversible structural phase transitions at easily accessible device temperatures in a special class of long-alkyl-chain-based hybrid inorganic-organic materials.[8,10,15]

The evolution of switching behavior of exciton is systematically explored in long alkyl chain based Inorganic Organic (IO) hybrids $(C_nH_{2n+1}NH_3)_2PbI_4$; n = 12, 16, and 18 (CnPI which are named as C12PI, C16PI and C18PI, respectively) and another system, similar to C12PI, $(NH_3C_{12}H_{22}NH_3)PbI_4$ (hereafter, DDPI). Systematic temperature-dependent confocal microscopic imaging, photoluminescence (PL) and transmission studies on thin films and single crystals are presented to establish a correlation between structural and optical exciton features. Understanding such thermo-optic switching of these hybrids is essential to pave the way for applications in photonic architectures.

II. EXPERIMENTAL DETAILS

Yellow single-crystals of CnPI (n = 12, 16, 18) and of DDPI were harvested from solution processing methods, as previously reported previously.[8,10,15,16] Several other 2D inorganic-organic hybrid multiple quantum wells (IO-MQWs) were also prepared from similar methods. Thin films were obtained by spin-coating a solution of CnPI and DDPI crystals dissolved in tetrahydrofuran (THF) and di-methyl sulfoxide (DMSO) solvents respectively.[8,10] PL and transmission measurements of both single crystals and thin films were carried out using a modified confocal microscope (FV1000, Olympus) with a temperature-controlled scanning stage and a spectrometer (HR2000). The spectrometer is coupled to the microscope to collect the white light transmission at local positions, with spectral span ranging from 300 nm to1000 nm, as well as the emitted PL (excited by a 447 nm CW diode laser, 30 mW) locally from a 3 μm spot. This system allows simultaneous recording of high-resolution images as well as PL and transmission spectra from an area of $\sim 1\ \mu m^2$.

III. RESULTS AND DISCUSSIONS

A. Structural phase transitions

Alkylammonium chain-based IO-hybrids in the generic form of $(C_nH_{2n+1}NH_3)_2PbI_4$ ($12 \leq n \leq 18$) are of special

[a)]Author to whom correspondence should be addressed. Electronic mail: pradphysics@gmail.com. Fax: +91(11) 2658 1114; Currently at Optoelectronics Research Centre, University of Southampton, Southampton, UK.

interest because of their unique optical properties. These hybrids show various temperature induced structural phases. One of the immediate observations of the phase-change is the dramatic color change[8] between yellow and orange, typically within a temperature cycle between 25 °C and 90 °C.

Single-crystal X-ray diffraction analysis (Single-crystal XRD)[8,10] revealed that these hybrids show a reversible phase transition within such device operating temperatures (25-90 °C): a stable phase (hereafter phase-I) at room temperature and an unstable phase at high-temperature (hereafter phase-II). Schematic crystal structures of both phases, for one of the hybrids C12PI, are shown in Figs. 1(a) and 1(b). The basic structure of these IO-hybrids, $(C_nH_{2n+1}\text{-}NH_3)_2PbI_4$ (n = 12, 16 and 18), consists of layers of corner-shared PbI_6 octahedra and bi-layers of organic cations stacked alternatively.[8] The side-linked PbI_6 octahedra are extended as 2D planar sheets and the PbI_6 octahedra of adjacent layers are coupled by two organic moieties via N-H···I weak hydrogen bonds through NH_3 ligands of the organic cations. While both low and high temperature phases (Phase I and II) have similar layered structures, the crystal packing are orthorhombic and monoclinic with corresponding space groups (P*bca*) and ($P2_1/a$) for phase-I and phase-II respectively.[8,15] Structural phase transitions can be considered to be a consequence

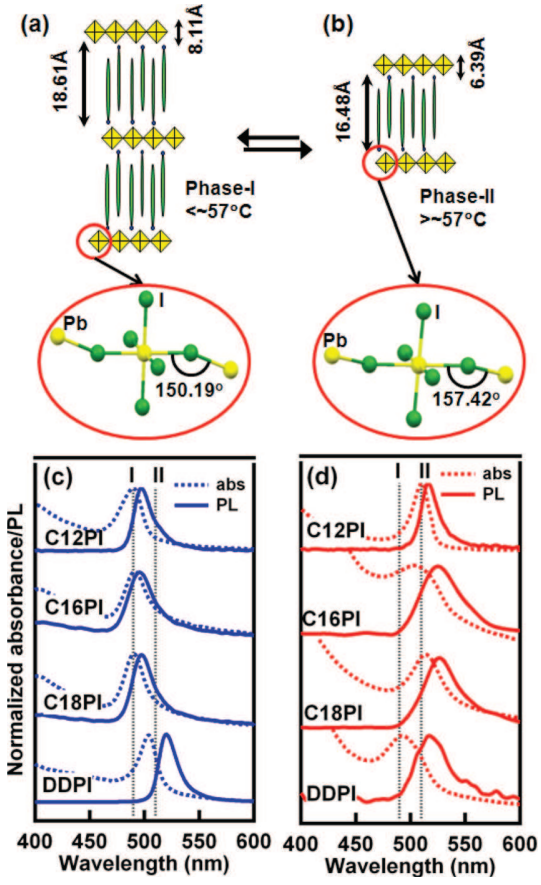

FIG. 1. (Color online) (a) and (b) Schematic crystal structures of C12PI phase-I and II, respectively. Inset shows the Pb–I–Pb atomic bonding within the inorganic network. (c) Phase-I and (d) Phase-II, exciton absorption (dotted line) and emission (solid line) spectra of C12PI, C16PI, C18PI and DDPI thin films. Gray lines are indicative of peak positions for phase I and II.

of conformational changes within the alkylammonium chains (organic cations), where the torsion angles around the N–C and/or C–C bonds change as the temperature increases. Another notable feature is that the PbI network layers are not completely planar but slightly crumpled, with Pb-I-Pb angles 150.19° (for phase-I) and 157.42° (for phase-II) (see inset of Figs. 1(a) and 1(b)). These features are the same for all long alkyl chain based IO-hybrids under study.[8,10,16]

The phase transition temperatures based on present and previous thermal and structural studies are[8,10,16]

$$\text{C12PI(I)} \underset{32.9\,^\circ\text{C}}{\overset{41.7\,^\circ\text{C}}{\rightleftharpoons}} \text{C12PI(II)} \underset{72.0\,^\circ\text{C}}{\overset{76.2\,^\circ\text{C}}{\rightleftharpoons}} \text{C12PI(III)}$$

$$\text{C16PI(I)} \underset{59.3\,^\circ\text{C}}{\overset{66.9\,^\circ\text{C}}{\rightleftharpoons}} \text{C16PI(II)} \underset{90.0\,^\circ\text{C}}{\overset{95.0\,^\circ\text{C}}{\rightleftharpoons}} \text{C16PI(III)}$$

$$\text{C18PI(I)} \underset{67.6\,^\circ\text{C}}{\overset{73.1\,^\circ\text{C}}{\rightleftharpoons}} \text{C18PI(II)} \underset{93.0\,^\circ\text{C}}{\overset{100\,^\circ\text{C}}{\rightleftharpoons}} \text{C18PI(III)}$$

$$\text{DDPI(I)} \underset{70.0\,^\circ\text{C}}{\overset{80.0\,^\circ\text{C}}{\rightleftharpoons}} \text{DDPI(II)}$$

Accordingly, there are two types of phase transition that can occur in these hybrids: The first (or pre-melting; phase-I to phase-II) transition exhibits considerable thermal hysteresis, showing prominent structural transformation, as evidenced by thermal, infrared and single crystal XRD studies.[8,10,16] The second (or melting; phase-II to phase-III) transition is accompanied by dilation of the lattice parameters. Recent and earlier reports on phase transitions indicate a clear dilation of crystal lattice during this second transition and loss of crystallinity which prevents the study of crystal structure.[8,16]

B. Temperature induced phase changes and corresponding exciton behavior

These IO-hybrids consist of 2D layered structure with inorganic semiconductor and organic layers stacked alternatively (Fig. 1(a)) and are regarded as a *natural multiple quantum well* (MQW) structure.[11,12] The '*well*' and '*barrier*' widths of these IO-hybrids were estimated from single crystal XRD analysis. The '*well*' width is ~6 Å for CnPIs and ~6.2 Å for DDPI and the '*barrier*' widths are typically 18 Å, 23 Å, 25.5 Å and 9.8 Å for C12PI, C16PI, C18PI and DDPI, respectively.

These IO-hybrid films show uniform layered arrangement and show strong room-temperature exciton absorption and PL (phase-I) at ~490 nm and ~500 nm, respectively, for CnPI thin films and at ~510 nm and 520 nm respectively for DDPI thin film (Fig. 1(c)). Both absorption and PL exciton line shapes are narrow with spectral widths less than 30 nm. At higher temperatures (phase-II), CnPIs excitons switch to higher wavelength regions with absorption peaks at ~510 nm and corresponding PL at ~520 nm (Fig. 1(d)). In contrast, DDPI exciton absorption switches to lower wavelength regions, ~495 nm with corresponding PL at ~516 nm (Fig. 1(d)). Nevertheless, both the phases of CnPI and DDPI preserve strong excitons with narrow bandwidths.

To understand the temperature induced phase changes and the corresponding exciton behavior, both transmission

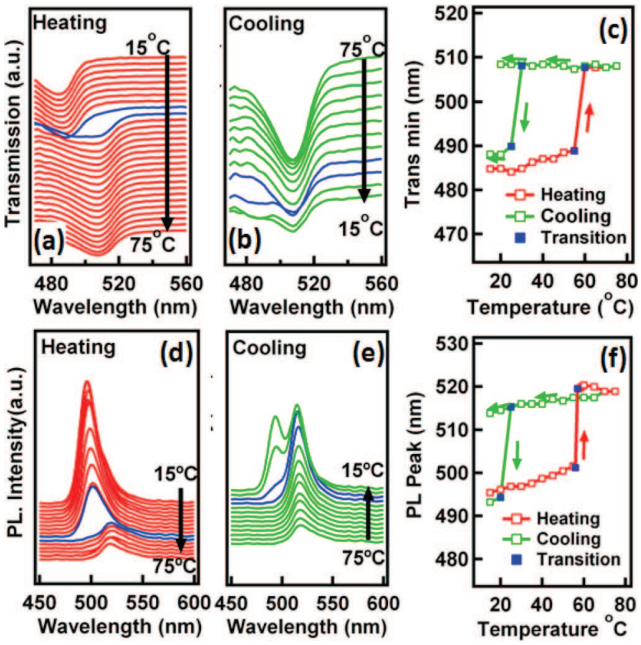

FIG. 2. (Color online) Transmission spectra of C12PI thin film (of thickness ~100 nm) during (a) heating and (b) cooling cycles between temperatures 15 °C and 75 °C. (d) and (e) are PL spectra of corresponding heating and cooling cycles. (c) and (f) are temperature dependence of transmission minima and PL peak maxima, respectively.

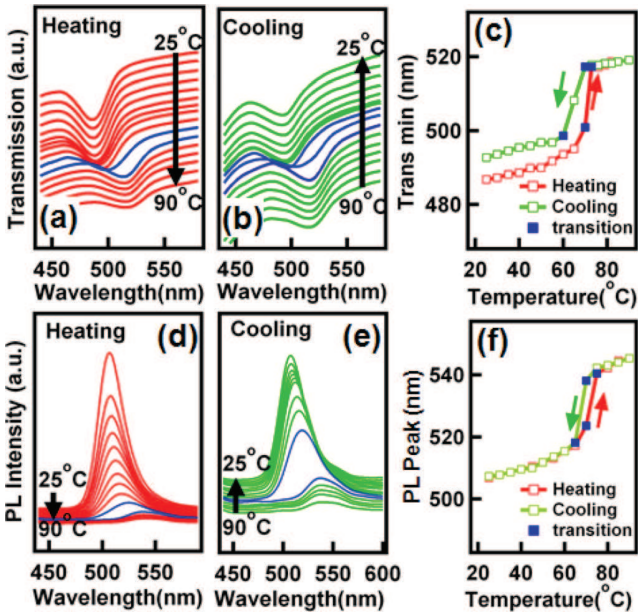

FIG. 3. (Color online) Transmission spectra of C16PI thin film (of thickness ~100 nm) during (a) heating and (b) cooling cycles between temperatures 25 °C and 90 °C. (d) and (e) are PL spectra of corresponding heating and cooling cycles. (c) and (f) are temperature dependence of transmission minima and PL peak maxima, respectively.

and PL spectra of CnPIs and DDPI thin films (thickness ~100 nm) were systematically monitored between 15 °C and 90 °C with 3 °C steps. Such phase change induced spectral changes of C12PI are shown in Fig. 2. Besides the exciton energy shift, it is also observed that the PL intensity of the phase-II exciton is three times less than phase-I. Extracting peak wavelengths corresponding to the maximum PL/transmission minima through a full temperature cycle is presented in Figs. 3(c) and 3(f). On cooling, the phase-II exciton persists even at room-temperature and remains for several hours. However, when these films are further cooled to 15 °C, phase-I appears along with phase-II and a complete recovery of phase-I only happens after several hours. We speculate that the inorganic layer crumpling is energetically favorable once many tens of QW layers have built up. Below this, the Peierls distortion is hampered by strain, leading to a metastable behavior in thin films.[15] As such, the exciton switching can be modified by the local nanoscale environment, providing innovative opportunities for device applications.

While the spectral switching of C16PI are close to that of C12PI, the phase transition temperature of C16PI is higher compared to C12PI. Temperature dependent transmission/PL spectra were monitored between 25 °C and 90 °C and are presented in Fig. 3. In the temperature range between 65 °C to 75 °C, the exciton peak switches from 500 nm to 540 nm. This switching is at ~75 °C during heating and ~65 °C during the cooling cycle. On comparing PL/transmission spectra of C12PI thin films (Fig. 2) to that of C16PI thin films (Fig. 3), the C16PI exciton swaps between these two phases within a smaller temperature span over a full temperature cycle. Annealing effects,[15] related to internal strain, are less dominant in C16PI as compared to C12PI, which accounts for the relatively narrow thermal hysteresis for C16PI observed. On close observations, high temperature PL of C16PI is comparatively broader and shifts toward longer wavelength (540 nm).

In the same vein, the temperature dependent PL/transmission spectra of C18PI (Fig. 4) shows exciton switching similar to that of C12PI but with higher switch-over temperatures, ~68 °C and ~78 °C. While the phase change temperatures of CnPI were same for transmission minima and PL peak maxima, the hysteresis curves show differences during cooling cycle (Figs. 2(c) and 2(f), 3(c), 3(f) and 4(c), 4(f)). In C18PI, the cooling/heating switch-over temperatures are very close (~10 °C) compared to C12PI (~40 °C). Such relatively narrow and complete thermal hysteresis suggests that the long alkyl chains help in retaining the Pb-I-Pb network to its natural crumpling with reduced annealing effects[15] related to internal strains. Furthermore, a reduced stokes shift (difference between transmission minima and PL maxima) was also observed for all CnPI (n = 12, 16 and 18) during cooling cycle. Annealing effects might have caused the PbI network to release its strain and hence in the suppression of non-radiative transition,[17] resulting in a reduced stokes shift. Further studies on annealing effects versus stokes shift would be interesting.

Exciton PL/transmission spectral features of DDPI thin films were recorded and analyzed over a temperature range of 25 °C to 90 °C for both heating and cooling cycles (Fig. 5). In DDPI, the exciton switching behavior is completely different to that of other CnPIs. DDPI thin films show strong room-temperature exciton transmission and PL peaks, relatively at higher wavelength side, at ~507 nm and ~520 nm, respectively. Upon heating, the PL maxima slowly switches to the *higher* energy side, i.e., from ~520 nm to ~516 nm at about 80 °C and switches back to ~520 nm during the cooling cycle. Similar switching is observed in transmission spectra. A

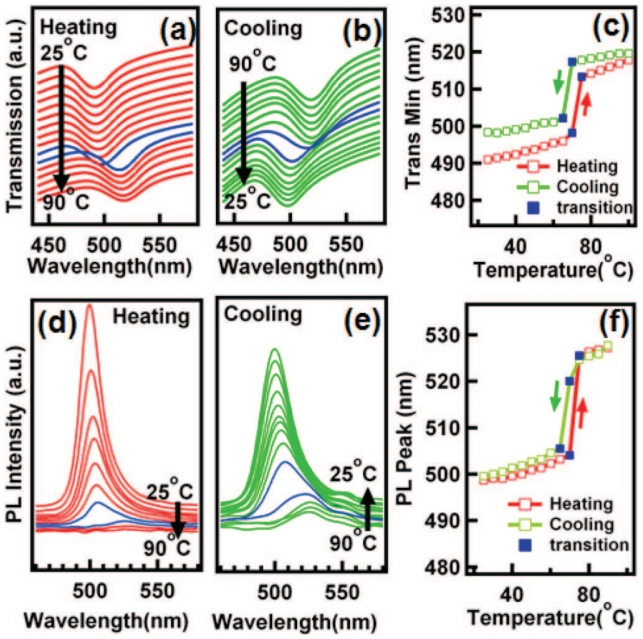

FIG. 4. (Color online) Transmission spectra of C18PI thin film (of thickness ~100 nm) during (a) heating and (b) cooling cycles between temperatures 25 °C and 90 °C. (d) and (e) are PL spectra of corresponding heating and cooling cycles. (c) and (f) are temperature dependence of transmission minima and PL peak maxima, respectively.

particular feature of the phase-change hysteresis of this exciton switching is its slowly varying nature: on heating, the PL maxima slowly increase from 520 to 525 nm with a rate of ~0.05 nm/°C and at the transition temperature (~80 °C), it rapidly switches to a lower-wavelength ~515 nm. This slowly varying nature and blue-shifted phase-change on heating is

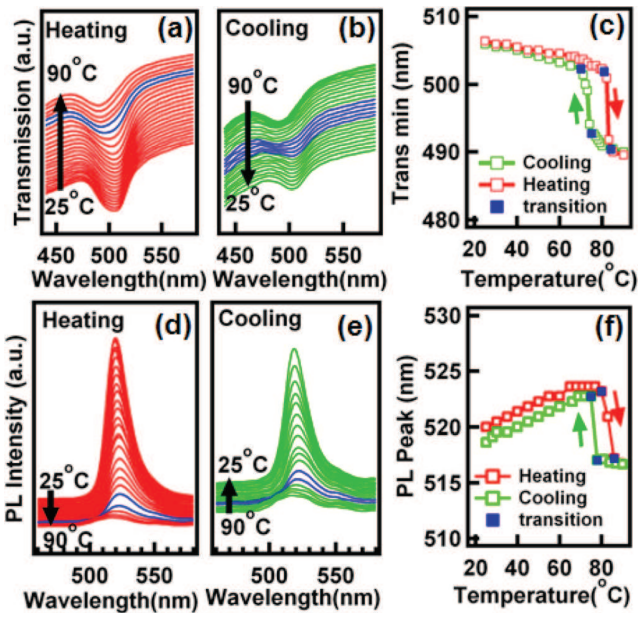

FIG. 5. (Color online) Transmission spectra of DDPI thin film (of thickness ~100 nm) during (a) heating and (b) cooling cycles between temperatures 25 °C and 90 °C. (d) and (e) are PL spectra of corresponding heating and cooling cycles. (c) and (f) are temperature dependence of transmission minima and PL peak maxima, respectively.

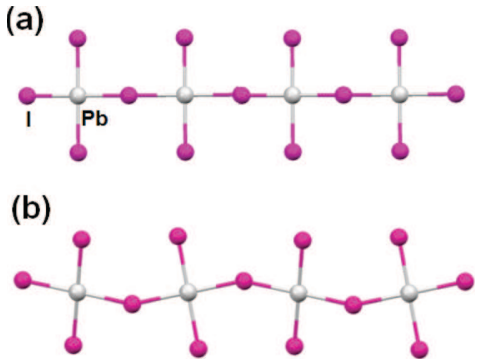

FIG. 6. (Color online) Schematic arrangement of Pb and I atoms in (a) DDPI and (b) C12PI. 2D layering of PbI network is perpendicular to the plane.

different to that of other alkyl-chained IO-hybrids (CnPIs, where n = 12, 16, and 18), where the exciton switching was entirely opposite, i.e. the PL maxima shifts toward the red end with a rate >0.11 nm/°C.

Fig. 6 shows the schematic representation of Pb-I-Pb network arrangement of DDPI and C12PI at room-temperature. In DDPI, the organic moiety (1,12-diaminododecane (DD)) is similar to that of C12PI, with the same number of carbon atoms in the alkyl chain as C12, but with amino groups at both the ends of the chain.[10] Due to the biterminal amino groups, the adjacent PbI layers in DDPI are coupled by a single organic, rather than two in the case of C12PI. As a consequence, the interlayer separation of DDPI (c ~ 16 Å) is smaller than C12PI (c ~ 24 Å).[8,10,15] Moreover, the corner shared I atoms in DDPI are in-plane with perfect ordering and less distorted in the I-Pb-I *cis* and *trans* angles[10] (see Fig. 6(a)) whereas in C12PI, the Pb-I network is more disordered[8,15] (see Fig. 6(b)).

The Pb-I-Pb in-plane bonding in DDPI is of a more planar nature, similar to that of other reported IO-hybrids $(C_6H_5C_2H_4NH_3)_2PbI_4$ (PAPI) and $(C_6H_9C_2H_4NH_3)_2PbI_4$ (CHPI).[6,7] Similarly the high-temperature-phase exciton energy (2.4 eV) is closer to our earlier reported IO-hybrids of more crumpled PbI structures, $(Cl\text{-}C_6H_4NH_3)_2PbI_4$ (CAPI)[14] and room-temperature C12PI (Fig. 6). Therefore, we infer that during the phase transition, PbI layers of DDPI switch from stable planar structure to more crumpled structure,[13,14,18,19] and as a consequence, the room-temperature exciton PL is at higher wavelength, ~520 nm, compared to other alkyl-chain based hybrids (CnPIs). However, high temperature crystal structure of DDPI is essential to understand such structural comparison. In our recent communication, by studying exciton PL from a number of similar 2D layered hybrids with different organic moieties, a correlation was established between the exciton energies and the Pb-I-Pb in-plane bonding angle.[15] This confirmed the key relationship between crumpling of inorganic layers and the exciton energies, separate from other influential factors such as dielectric confinement and barrier/well widths.

Despite some understanding of the dependence of exciton energies on other factors such as inorganic and organic layer sizes and the dielectric contrast between them,[11,12] a quantitative theoretical estimates of exciton energies remain

out of reach. According to single crystal XRD information,[8] CnPIs lattice spacing at room temperature (c = 49.03, 59.29, 64.45 Å for n = 12, 16, and 18 respectively) monotonically increase with increase in the alkyl chain length. However, the experimental room-temperature absorption and emission exciton energies (2.51 eV and 2.52 eV) do not show any variation with respect to an increase in organic chain length. This may arise from the layer crumpling, as seen from Pb-I-Pb bending angles, which are very close in these compounds (150.19°, 149.52° and 149.39°, respectively). However, they show less crumpling effect (with Pb-I-Pb bond angles 158.83°, 158.41° and 157.42°) at high-temperatures. Due to less crumbling, the exciton energy shift toward the red end was only about 0.2 eV.

In general, from the present and previous structural, thermal and spectroscopic studies, phase changes in these alkyl chain based IO-hybrids lead to many structural deformations, that includes (1) an increase in the disorder of the alkyl chain orientation, (2) changes in the crystal structure, (3) deformations of the inorganic (PbI) network, and (4) spatial shifts in the coupling between the ammonia group of the organic moiety and the PbI network.[8,10,15]

C. Distinct exciton behavior in C16PI crystals

As a general observation, both single crystals and thin films show two types of excitons at high and low temperature within the temperature range of 25 °C to 90 °C. The phase transition temperatures increase with increasing alkyl chain length in CnPI, which clearly supports the structural observations. However, the phase transitions observed from the optical measurements are different for thin films and single crystals and cannot be directly compared with values obtained from DSC studies.[8] While structural measurements solely monitor the structural modification, the exciton PL and transmission are critically dependent on film thickness, layered arrangement and morphology,[14,15] hence changes can be expected when looking at single crystals.

While the PL spectra of single crystal C12PI and C18PI show clearly two kinds of phases during heating and cooling cycles, the C16PI crystal shows more than one phase at high temperatures, between 70 °C and 90 °C. To further monitor these high temperature phases, spatial spectral scanning of a C16PI crystal is performed across 1 mm^2 areas with 20 μm resolution at temperatures 25 °C and 70 °C (experimental details are given in Sec. II).

Fig. 7 shows the PL spectra scanned along a single crystal (indicated by a broken line in Fig. 7(a)) with a step size of 0.02 mm. The PL line scan has been performed at 25 °C, 70 °C and again after cooling at 25 °C (Figs. 7(c)–7(e)). As seen, four kinds of PL spectra are observed which are peaked at 497, 520, 545 and 615 nm, named as I, II, III and IV, respectively (Fig. 7(b)). While phase-I PL is related to the room-temperature phase (25-60 °C), other peaks, II, III and IV, are from high temperature phases. Phase II and III are close to each other and spectrally overlap. We note that the phase-I exciton emission is almost an order of magnitude stronger than II and III and two orders of magnitude stronger than phase-IV. While the spectral widths of I, II and III are

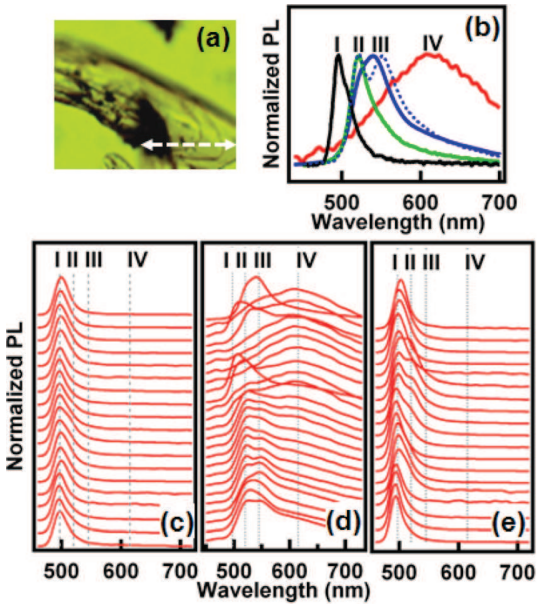

FIG. 7. (Color online) (a) Confocal image of C16PI crystal. (b) Normalized exciton PL spectra at different temperature-dependent phases I, II, III and IV. Dotted line (blue) shows the co-existence of phase-II and -III. (c) - (e) Normalized PL spectra scanned along the white dotted line (shown in Fig. 7(a)), with step size 0.02 mm, recorded at (c) 25 °C, (d) 70 °C and after cooling to (e) 25 °C. Spectra recorded at various distances are shifted up the *Y*-axis for clarity.

quite narrow (FWHM ~ 30 nm), the PL corresponding to IV is much broader with an FWHM of ~100 nm.

The notable observations from these temperature dependent studies are:

(i) The narrow and intense PL (~500 nm) observed at room-temperature is related to the room temperature excitons and of phase-I, similar to C12PI.

(ii) Another narrow PL line observed at 520 nm at high temperature, which is related to the phase II exciton, is an order of magnitude weaker than phase-I intensity.

(iii) High temperature (78 °C) exciton PL is composed of two overlapping distinct narrow peaks at 520 nm and 540 nm. The narrow linewidth at 540 nm could possibly be from the excitons from another higher-order metastable phase (phase-III), in accordance with earlier thermal and structural studies.[8,16] However, this phase is associated with a melting transition (~95 °C) and therefore can show loss of crystallinity as well as dilation of the crystal lattice. The possibility of structural deformations within phase-II structures might also result in these red-shifted high temperature excitons.

(iv) PL exciton switching is clearly visible as in the case of other CnPI crystals, similar to that of thin films.

(v) The PL at 615 nm is of very low intensity (almost two orders of magnitude weaker than phase-I) and spectrally broad (FWHM ~ 100 nm). This PL could be due to crystal defects, caused by uneven packing of inorganic-organic layers at the crystal edges.[14]

The confocal microscope image and the spatial PL morphology of C16PI crystals extracting the PL spectra of all

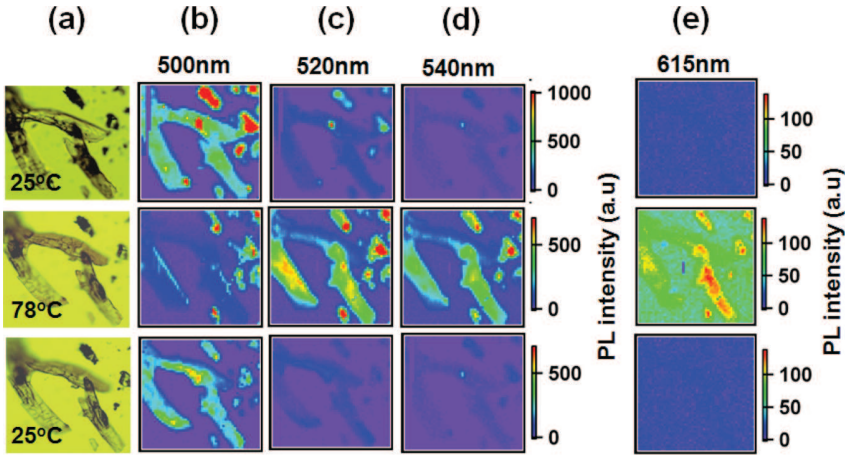

FIG. 8. (Color online) (a) Confocal images of C16PI crystals recorded at 25 °C and 78 °C again at 25 °C after cooling. (b)-(e) are PL mappings recorded at exciton PL wavelengths (b) 500 nm, (c) 520 nm, (d) 540 nm, and (e) 615 nm for corresponding temperatures.

these phases are presented in Fig. 8. The crystal color changes (Fig. 8(a)), visible to the naked eye, between light yellow to orange color when the temperature is increased from 25 °C to ~78 °C (vice versa on cooling) reveals the switching of optical excitons from phase-I ($\lambda_{PL} = 497$ nm) to phase-II/III ($\lambda_{PL} = 520$ nm and 540 nm, and vice versa). At 25 °C, the PL is completely in phase-I, and similarly at 78 °C, the PL from phase-I completely disappears and the PL arises only from phase-II and III excitons. When the temperatures are reduced back to room-temperature, the PL switches back to phase-I. Weak PL at λ~520 nm at 25 °C (Fig. 8(c)) is not from high temperature phase excitons but is only due to the extended spectral wings of the 500 nm peak which has a finite intensity at 520 nm.

IV. CONCLUSION

In conclusion, exciton switching in phase-change hybrids $(C_nH_{2n+1}NH_3)_2PbI_4$ (n = 12, 16 and 18) and $(NH_3C_{12}H_{22}NH_3)PbI_4$ was systematically explored. Two structural phases found between 15 °C and 90 °C, based on orthorhombic and monoclinic unit cells, show different optical excitons which are demonstrated to arise from the reversible crumpling of the quantum well layers. Thermal cycling experiments on exciton PL and transmission reveals complete reversibility of the phase transitions in these phase change hybrids. However, depending on structural features such as the length of alkyl chains and available amino groups, they show distinct thermal hysteresis behaviors. Such detailed understanding of the exciton behavior is essential for optoelectronic devices, such as switchable microcavity strong-coupling devices and nonlinear optical switches.[5] Further controlling the exciton switching by external electric fields can potentially pave the way to new generations of electro-optic and all-optical devices.[20]

ACKNOWLEDGMENTS

This work is part of the *UK-India Education and Research Initiative* (UKIERI) program, and High-Impact Research Scheme of IIT Delhi. The technical help from Mr. G. Sharachandra Yadav, IIT Delhi is appreciated.

[1]C. R. Kagan, D. B. Mitzi, and C. Dimitrakopoulos, Science **286**, 945 (1999).
[2]T. Dantas de Morais, F. Chaput, K. Lahlil, and J. P. Boilot, Adv. Mater. **11**, 107 (1999).
[3]M. Era, S. Morimoto, T. Tsutsui, and S. Saito, Appl. Phys. Lett. **65**, 676 (1994).
[4]D. B. Mizi, K. Chondroudis, and C. R. Kagan, IBM J. Res. Dev. **45**, 29 (2001).
[5]K. Pradeesh, J. J. Baumberg, and G. Vijaya Prakash, Opt. Exp. **17**, 22171 (2009).
[6]D. G. Billing, Acta Crystallogr., Sect. E: Struct. Rep. Online **58**, m669 (2002).
[7]D. G. Billing and A. Lemmerer, Acta Crystallogr., Sect. B: Struct. Sci. **B63**, 735 (2007).
[8]D. G. Billing and A. Lemmerer, New J. Chem. **32**, 1736 (2008).
[9]G. Lanty, A. Bréhier, R. Parashkov, J. S. Lauret, and E. Deleporte, New J. Phys. **10**, 065007 (2008).
[10]K. Pradeesh, G. Sharachandra Yadav, M. Singh, and G. Vijaya Prakash, Mater. Chem. Phys. **124**, 44 (2010)
[11]T. Ishihara, J. Takahashi, and T. Goto, Phys. Rev. B **42**, 11099 (1990).
[12]T. Ishihara, J. Takahashi, and T. Goto, Solid State Commun. **69**, 933 (1989).
[13]K. Pradeesh, J. J. Baumberg and G. Vijaya Prakash, Appl. Phys. Lett. **95**, 033309 (2009).
[14]G. Vijaya Prakash, K. Pradeesh, R. Ratnani, K. Saraswat, M. E. Light, and J. J. Baumberg, J. Phys. D: Appl. Phys. **42**, 185405 (2009).
[15]K. Pradeesh, J. J. Baumberg, G. Vijaya Prakash, Appl. Phys. Lett. **95**, 173305 (2009).
[16]S. Barman, N. V. Venkataraman, S. Vasudevan, and R. Seshadri, J. Phys. Chem. B **107**, 1875 (2003).
[17]M. Albrecht, V. Grillo, T. Remmele, H. P. Strunk, A. Yu. Egorov, Gh. Dumitras, H. Riechert, A. Kaschner, R. Heitz, and A. Hoffmann, Appl. Phys. Lett. **81**, 2719 (2002).
[18]T. Hattori, T. Taira, M. Era, T. Tsutsui, and S. Saito, Chem. Phys. Lett. **254**, 103 (1996).
[19]X. Hong, T. Ishihara, and A. V. Nurmikko, Phys. Rev. B **45**, 6961 (1992).
[20]G. Grosso, J. Graves, A. T. Hammack, A. A. High, L. V. Butov, M. Hanson, and A. C. Gossard, Nat. Photonics **3**, 577 (2009).